Chlorophylls. IX. The first phytochlorin–fullerene dyads: synthesis and conformational studies

Juho Helaja,[ab] Andrei Y. Tauber,[ac] Yvonne Abel,[d] Nikolai V. Tkachenko,[c] Helge Lemmetyinen,[c] Ilkka Kilpeläinen[b] and Paavo H. Hynninen*[a]

[a] *Department of Chemistry, PO Box 55, University of Helsinki, FIN-00014 Helsinki, Finland*
[b] *Institute of Biotechnology, PO Box 45, University of Helsinki, FIN-00014 Helsinki, Finland*
[c] *Institute of Materials Chemistry, Tampere University of Technology, PO Box 541, FIN-33101 Tampere, Finland*
[d] *Institut für Organische Chemie, FB2, Universität Bremen, Leobener Str. NW2, D-28359 Bremen, Germany*

Received (in Lund) 9th April 1999, Accepted and transferred from Acta Chem. Scand. 16th June 1999

The first chlorin–fullerene electron donor–acceptor (DA) compounds have been synthesized. The synthesis produced C-2′ *R* and *S* epimers, both of which exhibited atropisomerism regarding the mutual orientation of the fullerene ball and the propionic acid residue of the phytochlorin unit. The atropisomerism arises from the short linkage between the C_{60} ball and the chlorin ring, which hinders free rotation of the bulky ball. Dynamic ^{1}H NMR and molecular modelling were used in concert to investigate the atropisomerism in the metal-free DA molecules **5**. The dynamic NMR-measurements showed a lower energy barrier [E_a = 21.4(5) kcal mol^{-1}] for one stereoisomer and a higher one [E_a = 23.0(8) kcal mol^{-1}] for the three other stereoisomers. MM+ molecular mechanic calculations were performed for each C-2′ epimer to assess the potential energy as a function of the angle of rotation about the C3–C2′ single bond. For the C-2′ *R* and *S* epimers, these calculations produced two potential energy curves that showed a near mirror-image relationship. Solvation phenomena were proposed to play an essential role in the stabilization of the isomers. Fast intramolecular photoinduced electron transfer from the chlorin donor to the fullerene acceptor was observed in polar solvents.

A wide range of complex molecular systems that absorb light and undergo photoinduced energy and electron transfer have been synthesized and studied.[1] A majority of these systems employ porphyrins or chlorins as electron donors and quinones as electron acceptors for mimicry of photosynthetic reaction centres. Recently, there have appeared new and attractive building blocks to be used as electron acceptors, the fullerenes. Several groups have already prepared and examined some donor-linked fullerenes including porphyrin-fullerene DA compounds.[2–4] However, there have been no reported structures consisting of a fullerene, covalently linked to a chlorin molecule. The chlorin linked systems would be of great interest, since the excitation possibility at the chlorin long-wavelength Q-band, which is missing from the electronic spectrum of fully conjugated porphyrins, enables the achievement of higher quantum yields in solar energy conversions.[5,6] The chlorins are known to possess a variety of photophysical[7] and electrochemical properties,[8] which provide an opportunity to tune the energetics of photoinduced charge separation. Here we shall describe the synthesis and conformational studies of the first phytochlorin–fullerene DA compounds, which contain a chlorophyll derivative, phytochlorin, as the donor.

Results and discussion

Our synthetic pathway (Scheme 1) starts from chlorophyll *a* (**1**), which was pyrolyzed to produce 13^2-demethoxycarbonylchlorophyll *a* (pyroChl *a*).[9] After transesterification of pyroChl *a* with 5% H_2SO_4 in MeOH, the vinyl group of the produced 3^1,3^2-didehydrophytochlorin methyl ester (**2**) was oxidized into a formyl group by adding OsO_4 and $NaIO_4$ successively *in situ*[10] to give the methyl ester of 3-deethyl-3-formylphytochlorin (**3**) in a yield of 57% relative to chlorophyll *a*. For the coupling of fullerene (C_{60}) with phytochlorin **3**, the method of Prato and co-workers[11] was employed. This method involves the addition of a reactive azamethine ylide across a juncture of two 6-rings in the fullerene. Thus, the reaction of **3** with C_{60} and *N*-methylglycine in refluxing toluene gave, after column chromatography, the 2′-epimeric compounds **6** in a yield of 49% relative to the phytochlorin **3**. Stirring of **6** with $Zn(OAc)_2$ in $CHCl_3$–MeOH metalated the phorbin ring, resulting in the Zn–phytochlorin–fullerene compounds **7**. For the preparation of compounds bearing a free propionic acid residue, the methyl ester of 3-deethyl-3-formylphytochlorin (**3**) was subjected to an acid hydrolysis, producing 3-deethyl-3-formylphytochlorin (**4**). The latter was coupled with C_{60} and *N*-methylglycine in refluxing 1,4-dioxane–toluene to give, after purification, **5** in a 38% yield relative to phytochlorin **4**.

The ^{1}H NMR spectra of **5** in $CDCl_3$–CD_3OD mixture (40 : 1, v/v) revealed the presence of four different molecular species in the solution. These species represent a pair of diastereomers and a pair of atropisomers of each diastereomer, differing in the orientation of the fullerene ball with respect to the propionic acid side-chain of the chlorin ring (Fig. 1). The atropisomerism arises from the short linkage between the C_{60} ball and the chlorin ring, which restricts free rotation of the bulky ball. Further silica gel chromatography of compounds **5** enabled the separation of two components, **PF1** and **PF2**. These were identified by ^{1}H NMR as two different atropisomers, each comprising a pair of diastereomers, epimeric at position 2′ of the pyrrolidine ring. The atropisomerism was discovered on the basis of the slow conformational exchange between **PF1** and **PF2** observed at room temperature. The complete assignment of the ^{1}H NMR spectra could be achieved for each of the four isomers by applying the ^{1}H NMR ROESY technique.[12] Thus it was possible to study both the structural features and the atropisomerism for each isomer separately.

In the detailed analysis of the ^{1}H NMR spectra, some

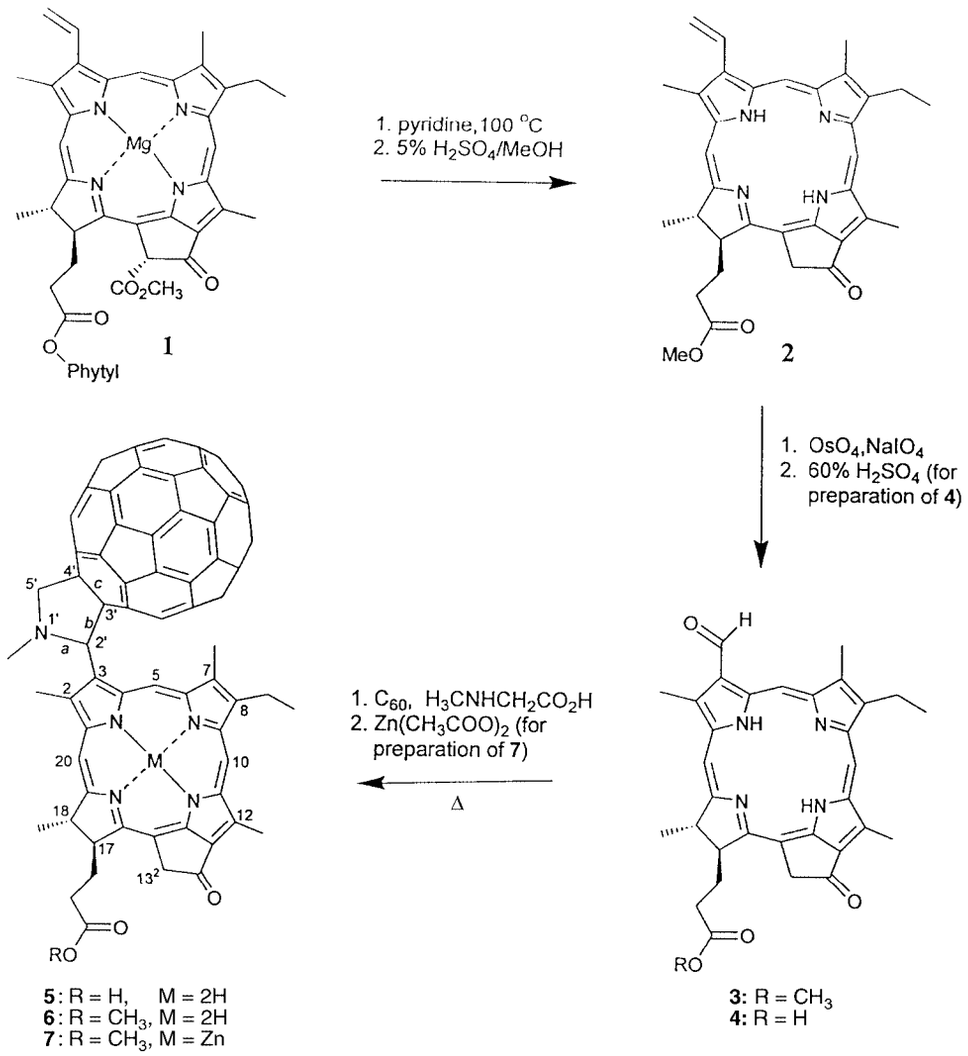

Scheme 1

unusual chemical shifts were observed for both atropisomers **PF1** and **PF2**. The inspection of the $\Delta\delta_H$-values in Fig. 2 indicates that the fullerene ball induces different shielding and deshielding effects on the chlorin ring protons depending on their proximity. The 5-C*H* resonance of the chlorin ring is markedly shifted downfield ($\Delta\delta \sim 2$) for one epimer of each atropisomer (denoted as **PF1***A* and **PF2***B*, where *A* and *B* stand for the 2′-epimers), whereas for the other epimer (**PF1***B* and **PF2***A*), the 5-C*H* δ-value is similar to that of phytochlorin **2**.[13] On the other hand, the δ-values of the 2^1 methyl protons show marked downfield shifts ($\Delta\delta \sim 0.5$) for the **PF1***A* and **PF2***B* isomers, but smaller ones ($\Delta\delta \sim 0.1$) for the **PF1***B* and **PF2***A* isomers. The substantial downfield shifts occur due to the deshielding effect of the C_{60} pentagon rings[14] and indicate that, in **PF1***A* and **PF2***B*, the fullerene ball is located close to the 5-C*H* of the chlorin ring. The average C_{60} effect is deshielding, because the shielding arising from the hexagon ring is weaker than the deshielding from the pentagon ring.[14] Further, it is noteworthy that, in the **PF1***B* and **PF2***A* isomers, the 7^1 methyl group is clearly more shielded ($\Delta\delta = -0.12$ and -0.16). This shielding effect is very likely caused by the proximity of the C_{60} hexagon ring(s).

The foregoing conclusions are corroborated by the correlations observed in the ROESY spectra, which revealed the spatial proximity of the 2′-C*H* of the pyrrolidine ring and the 5-C*H* proton in the **PF1***B* and **PF2***A* isomers. In case of **PF1***A* and **PF2***B*, the same ROESY correlations were absent, but instead a correlation between the 2′-C*H* and 2^1-CH_3 protons was observed. The information provided by the ROESY experiments was used for constructing molecular models for each of the four isomers. The inspection of the models revealed unambiguously that *A* and *B* are different epimers, whereas **PF1** and **PF2** are different atropisomers. However, the relatively high symmetry of the epimers and the large distance between the C-2′ and the other chiral centres in the molecule did not allow us to define experimentally the absolute stereochemistry at the C-2′ of each epimer.

In order to evaluate the energy barrier for the conversion from one atropisomer to another, the dynamic NMR investigation of **PF1** and **PF2** in $CDCl_3$–CD_3OD (40 : 1, v/v) mixture was performed. Fig. 3 presents the Arrhenius plots[15] for the interconversions between the isomers. The points on each plot represent the natural logarithm of the conversion rate constant *versus* inverse temperature. The rate constants were obtained from the one-exponential fitting of the points representing the integration values of the 10-C*H* signals *versus* time at different temperatures. Three of the straight lines are nearly parallel within the experimental error limits and their slopes give an activation energy (E_a) of 23.0(8) kcal mol^{-1}, while the filled-circle line (epimer *B* of **PF2**) affords a lower E_a of 21.4(5) kcal mol^{-1}. Molecular modelling was employed to trace the reason for this difference.

Two energy minima were found for the C-2′ *R*- and *S*-epimers: one for the α- and another for the β-atropisomer. The MM+ molecular modelling method[16] was used to assess the rotation barriers between the isomers, utilizing the fact that the motion of the fullerene ball from one side of the chlorin plane to its other side can only occur as a consequence of rotation

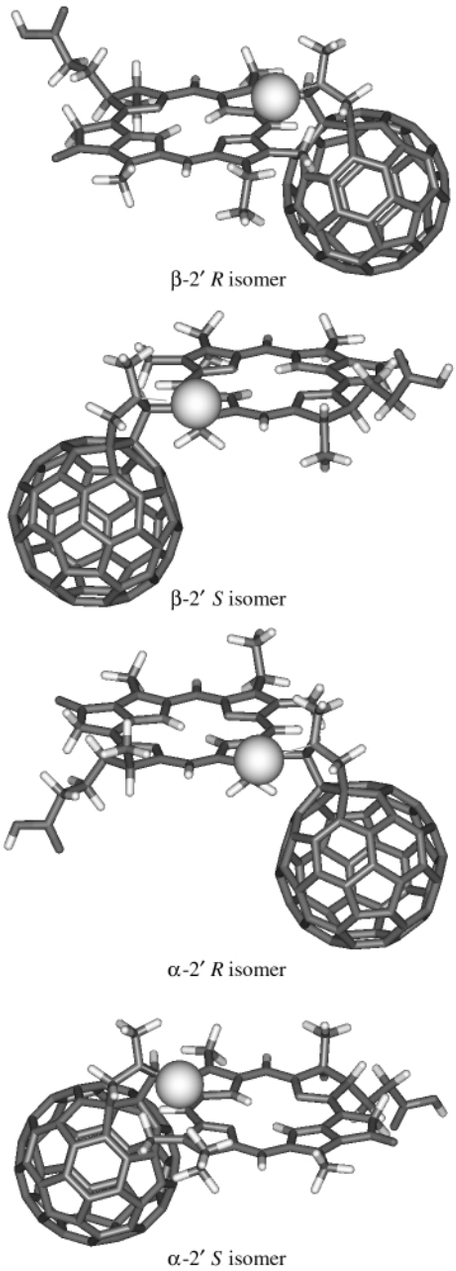

Fig. 1 The AM1 (RHF) energy optimized[12] capped-stick structures for the α- and β-atropisomers of the 2′-*S*- and *R*- epimers. The space-filling hydrogen atom is attached after optimization at the hydrogen-bonding distance (3 Å) using a pyramidal angle of 106° for pyrrolidine nitrogen.

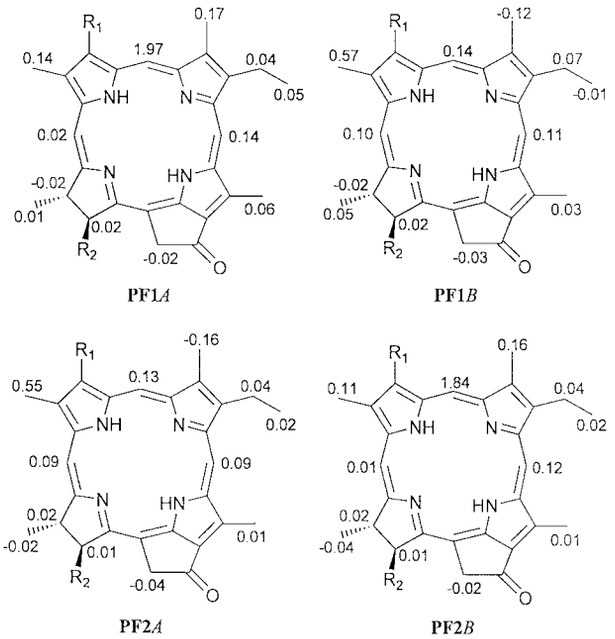

Fig. 2 The $\Delta\delta_H$-value maps for the chlorin part of the four isomers. $\Delta\delta_H = \delta_H$ (isomer) − δ_H (pyropheophorbide *a* methyl ester).[13]

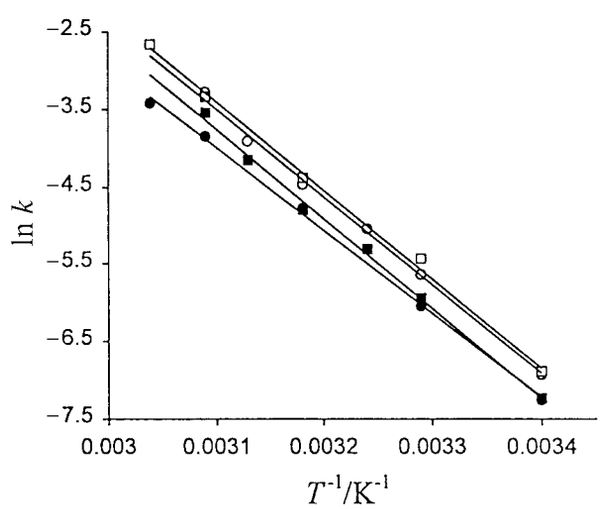

Fig. 3 The Arrhenius plots for the interconversions between the isomers. The hollow and filled symbols represent the **PF1** and **PF2** atropisomers, respectively. The square symbols correspond to the 2′-epimer *A* and the circle symbols to the 2′epimer *B*.

about the C3–C2′ single bond. The points on the curves (Fig. 4) were obtained by changing the torsion angle Θ (C4–C3–C2′–C3′) with 5° steps and optimizing the rest of the structure. The stepwise optimization was started from the α- and β-minimum conformations, proceeding with separate increments for clockwise and anticlockwise rotations. When the lowest energy value (E) was presented as a function of the corresponding torsion angle (Θ), the curves in Fig. 4 were obtained. In this way, the possible imperfections of the used optimization algorithm were made negligible. Thus, each point on the curves represents the global energy minimum for the corresponding torsion angle Θ.

The MM+ energy barriers (18–23 kcal mol^{-1}) between the minima in Fig. 4 are comparable to those measured experimentally. The energy curves show that the rotation energy barriers for the epimers are almost mirror images of one another. The inspection of the rotation energy minima suggests that the 2′*R* epimer favours the α-atropisomer ($\Theta = 280°$) and 2′*S* epimer the β-atropisomer ($\Theta = 75°$). The semiempirical AM1 modelling method[17] with restricted Hartree–Fock (RHF) spin-pairing option produced energy relations for the α- and β-minima of the C-2′*R* and *S* epimers, which are similar to those provided by the MM+ method (Fig. 4). For the β-2′*S* isomer, the heat of formation was $\Delta H_f = 1004.85$ kcal mol^{-1}, whereas for the α-2′*S* isomer the energy was 1.11 kcal mol^{-1} higher. The ΔH_f value of the α-2′*R* isomer was found to be lower by 0.76 kcal mol^{-1} ($\Delta H_f = 1005.09$ kcal mol^{-1}) than that of the β-2′*R* isomer ($\Delta H_f = 1005.85$ kcal mol^{-1}). Furthermore, the MM+ curve in Fig. 4 shows that the levels of the rotation energy barriers are rather similar for the 2′*R* and *S* epimers. Thus, based on the molecular modelling results *in vacuo*, it seems that the long distance from the C-2′ to the C-17 and C-18 chiral centres in the dyad molecules obscures the diastereomeric nature of these structures.

In solution, we expect that solvation interactions will contribute to the experimentally observed E_a-values. This contribution is likely to be different for different isomers. One possibility is that the electron lone-pair of the pyrrolidine nitrogen, vicinal

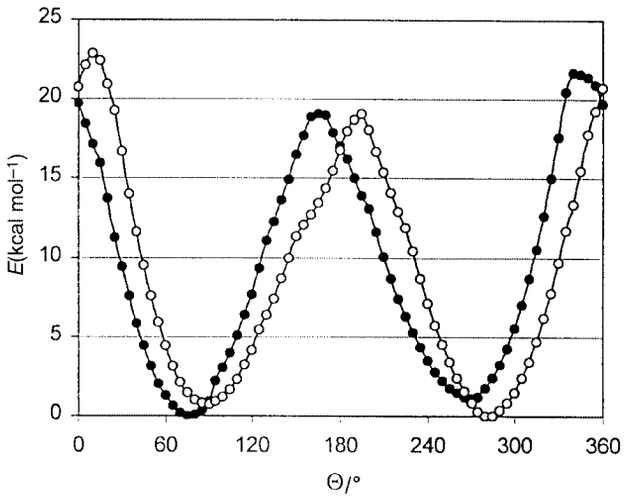

Fig. 4 The calculated energy curves for the rotation of the fullerene ball about the C3–C2′ single bond; filled circles: 2′-*S*-epimer, hollow circles: 2′-*R*-epimer. The points on the curves were obtained by changing the torsion angle *Θ* (C4–C3–C2′–C3′) with 5° steps and optimizing the rest of the structure using the molecular mechanics MM+ force field.[16]

to the chiral C-2′, will affect crucially the solvation stabilization of the atropisomers by forming a hydrogen bond to the solvent. In the AM1 optimized structures of the isomers (Fig. 1), we attached a hydrogen atom at the hydrogen-bonding distance to the pyrrolidine nitrogen in order to see whether this bonding is likely to occur. For the energy-minimized structures of the α-2′*R* and β-2′*S* isomers, the electron lone-pair is protected from the H-bonding contacts with solvent molecules by the 2^1 methyl group. In contrast, in the energy-minimized structures of the β-2′*R* and α-2′*S* isomers, the electron lone-pair is readily available for interactions with solvent molecules, thus making the hydrogen bonding *e.g.* to methanol possible. Moreover, in the β-2′*R* isomer, the C-17 propionic acid residue is on the same side of the chlorin ring plane as the pyrrolidine-*N* lone-pair orbital and could therefore contribute to the stabilization of the electron lone-pair *via* a through-space effect mediated by a chain of hydrogen bonded solvent molecules. According to the molecular modelling, the solvation stabilization in the α-2′*R* and β-2′*S* isomers seems energetically less favourable, whereas the stabilization may be more effective in the β-2′*R* isomer. The foregoing inspection led us to the conclusion that the α-2′*S* isomer (Fig. 1) is likely to be the fastest converting one.

The electron transfer properties of DA compounds **5**, **6** and **7** were investigated using time-resolved fluorescence and transient-absorption spectroscopies. A very fast electron transfer was observed between the D and A in polar solvents such as THF and benzonitrile. Thus, the rate constant of photoinduced electron transfer for **7** in THF solution was ~2×10^{12} s^{-1} with a lifetime of the charge-separated state close to 20 ps. The results of the fluorescence and transient-absorption studies in the NIR region (800–1000 nm) suggest that the energy transfer from the primary excited phytochlorin donor to the fullerene moiety occurs prior to the electron transfer.

The photochemical properties of the **PF1** and **PF2** atropisomers of the DA compounds **5**, were studied separately. These properties appeared to be virtually identical for both atropisomers in all solvents studied. This observation is in good agreement with our molecular modelling results, which suggest that the distance between the electron donor (phytochlorin unit) and the acceptor (fullerene unit) remains essentially the same in all isomers. The more detailed photochemical studies on the novel compounds, including the elucidation of the mechanism of the photoinduced electron transfer, is out of the scope of this paper and will be reported elsewhere.[18]

Experimental

The solvents used in the synthesis and separations were of analytical grade, and were dried and stored over 4 Å molecular sieves. Chloroform was distilled through a Vigreux-column prior to use. Silica gel 60 (230–400 mesh, ASTM, Merck, Darmstadt, Germany) was used for column chromatography.

The ^{1}H NMR spectra were obtained on a 300 MHz Varian INOVA for compounds **2**, **3**, **4**, **5** and **7** or on a Varian Unity 500 spectrometer for compound **6**. The sample volume was 0.6 ml in all measurements. The $CDCl_3$ used (Euriso-top, 99.96% D) was taken from ampoules and the CD_3OD (Fluka, 99.8% D) from a bottle. The ROESY NMR experiments were performed in order to accomplish the assignment of ^{1}H NMR spectra of the synthesized dyads. The mixing times used were 200–400 ms in the experiments. In other regards, the ROESY measuring conditions were essentially the same as those described in detail in our earlier paper.[12] The temperature calibrations in dynamic NMR were performed with ethylene glycol (100%, Varian test sample). The dynamic proton spectra were measured with an acquisition time of 3 s using a 2 s delay between the scans. The integration values of selected proton signals at each particular temperature were analysed as a function of time and the conversion rate-constants were calculated using Microcal Origin (4.1) software. The linear fittings of the Arrhenius plots were produced with the same software.

Molecular modelling was performed on Intel Pentium II 300 MHz (128 Mb RAM) utilizing HyperChem (release 4.5) software.[16] The full AM1 RHF optimization[17] of geometry was achieved using 445 molecular orbitals in the calculations. The AM1 structures were energy optimized employing the Polak–Ribiere conjugate gradient optimization algorithm with an energy convergence criterion of 0.01 kcal $Å^{-1}$ mol^{-1}. In the MM+ energy optimizations, the Newton–Raphson block diagonal optimization algorithm was utilized with the same energy convergence criterion. The stepwise torsion angle increments were achieved utilizing an EXCEL software.

The electronic absorption spectra were measured on a Varian Cary 5E UV–VIS–NIR spectrophotometer.

The matrix-assisted laser desorption–ionization time-of-flight mass spectrometry (MALDI-TOF) was performed in the positive ion delayed-extraction mode on a Bruker BIFLEX spectrometer, using a 337 nm nitrogen laser; α-cyano-4-hydroxycinnamic acid (0.1 M in THF–MeOH, 7 : 3) was used as a matrix.

Chlorophyll *a* (**1**) was isolated from clover leaves by the method described earlier,[19] modified for large-scale preparation. Buckminsterfullerene C_{60} (>98%) and *N*-methylglycine (sarcosine, >99%) were purchased from Fluka (Buchs, Switzerland).

13^2-Demethoxycarbonylpheophorbide *a* methyl ester (methyl pyropheophorbide *a*, 2)

Chlorophyll *a* (1.0 g) was quantitatively pyrolyzed by heating its degassed pyridine solution at 100 °C in a sealed tube, as described earlier.[9] The 13^2-demethoxycarbonylchlorophyll *a* was then demetallated and transesterified with 5% H_2SO_4 in MeOH (v/v) to produce methyl pyropheophorbide *a* (550 mg, 90% overall yield). The ^{1}H NMR and UV-VIS spectra of **2** were consistent with those reported earlier.[13]

3-Formyl-3-deethylphytochlorin methyl ester (3)

The vinyl group of methyl pyropheophorbide *a* (200 mg) was oxidized as described previously,[10] using OsO_4 and $NaIO_4$ *in situ*, to yield 130 mg (63%) of **3**. The spectral data were virtually identical with the reported ones.[10]

3-Formyl-3-deethylphytochlorin (4)

Compound **3** (25 mg) was dissolved in 25 ml of 60% (w/w) aqueous H_2SO_4 and the solution was stirred for 4 hours at

ambient temperature, protected from light. The reaction mixture was then poured into 300 ml of distilled water and 3-formyl-3-deethylphytochlorin (**4**) was extracted with CH_2Cl_2 (3 × 20 ml) until the water phase became colourless. The combined extracts were washed thoroughly with water to neutral pH, dried with Na_2SO_4 and evaporated to dryness on a rotary evaporator to yield 22 mg (91%) of **4**. ^{1}H NMR (300 MHz, $CDCl_3$): δ_H 11.47 (s, 3^1-C*H*), 10.18 (s, 5-C*H*), 9.50 (s, 10-C*H*), 8.80 (s, 20-C*H*), 5.31, 5.13 (AB spin system, $|^2J| = 20$ Hz, 13^2-CH_2), 4.55 (m, 18-C*H*), 4.38 (m, 17-C*H*), 3.73 (s, 2^1-CH_3), 3.65 (s, 12^1-CH_3), 3.64 (q, $^3J = 7.4$ Hz, 8^1-CH_2), 3.24 (s, 7^1-CH_3), 2.80–2.55, 2.45–2.20 (m, 17^1-CH_2, 17^2-CH_2), 1.85 (d, $^3J = 7.2$ Hz, 18^1-CH_3), 1.67 (t, $^3J = 7.4$ Hz, 8^2-CH_3), −2.15 (br s, 23-N*H*) (21-N*H* is not resolved); UV-VIS (CH_2Cl_2), λ_{max} (rel absorbance) 388 (0.857), 428 (1.000), 522 (0.149), 554 (0.159), 633 (0.086), 694 (0.772).

α,β-3-((2′*R*,*S*)-*N*-Methyltetrahydro[60]fullereno[*c*]pyrrol-2′-yl)-3-deethylphytochlorin (5)

Compound **4** (10 mg, 0.018 mmol) and *N*-methylglycine (8 mg, 0.09 mmol) were dissolved in a mixture of dry toluene (10 ml) and 1,4-dioxane (4 ml). A solution of 13 mg (0.018 mmol) of C_{60} in 15 ml of dry toluene was added to the reaction mixture, the mixture obtained was refluxed under Ar and the progress of the reaction was monitored by TLC on Merck's Si-60 plates [thickness of the layer 0.25 mm; eluent $CHCl_3$–MeOH 9 : 1 (v/v)]. After refluxing for 26 h, the mixture was cooled to room temperature, the solvents were evaporated off and the residue was chromatographed on a silica gel column [230–400 mesh; height of the layer 280 mm; 300 × 45 mm ID column; elution with $CHCl_3$–MeOH–CH_3COOH 20 : 1 : 0.01 (v/v)]. The main fraction was collected, washed with distilled water, dried over anhydrous Na_2SO_4 and evaporated to dryness on a rotary evaporator to give 9 mg (38% yield) of dyad **PF1**,**2**. The dyad was further chromatographed on another silica gel column [230–400 mesh; height of the layer 330 mm; 350 × 25 mm ID column; elution with $CHCl_3$–MeOH–CH_3COOH 30 : 1 : 0.01 (v/v)] providing two effluent fractions which were collected separately, washed with water and evaporated to dryness to yield atropisomer **PF1** (4 mg, 17%) and atropisomer **PF2** (5 mg, 21%) as mixtures of the 2′-*R*- and *S*-epimers. *Atropisomer* **PF1**: ^{1}H NMR (300 MHz, $CDCl_3$–CD_3OD 40 : 1), *Epimer A*: δ_H 11.38 (s, 5-C*H*), 9.53 (s, 10-C*H*), 8.58 (s, 20-C*H*), 6.39 (s, 2′-C*H*), 5.45 (AX spin system, d, $|^2J| = 9.7$ Hz, 5′-CH_2), 5.25, 5.10 (AB spin system, $|^2J| = 20.1$ Hz, 13^2-CH_2), 4.62 (AX spin system, d, $|^2J| = 9.7$ Hz, 5′-CH_2), 4.47 (m, 18-C*H*), 4.32 (m, 17-C*H*), 3.72 (overlapping quartets (oq), 8^1-CH_2), 3.68 (s, 12^1-CH_3), 3.55 (s, 2^1-CH_3), 3.41 (s, 7^1-CH_3), 3.05 (s, 1′-NCH_3), 2.74–2.50, 2.40–1.98 (m, 17^1-CH_2, 17^2-CH_2), 1.83 (d, $^3J = 7.3$ Hz, 18^1-CH_3), 1.75 (overlapping triplets (ot), 8^2-CH_3), −1.77 (br s, 23-N*H*) (21-N*H* is not resolved); *Epimer B*: δ_H 9.64 (s, 5-C*H*), 9.50 (s, 10-C*H*), 8.66 (s, 20-C*H*), 6.77 (s, 2′-C*H*), 5.32 (AX spin system, d, $|^2J| = 9.7$ Hz, 5′-CH_2), 5.23, 5.09 (AB spin system, $|^2J| = 20.1$ Hz, 13^2-CH_2), 4.65 (AX spin system, d, $|^2J| = 9.7$ Hz, 5′-CH_2), 4.47 (m, 18-C*H*), 4.32 (m, 17-C*H*), 3.99 (s, 2^1-CH_3), 3.75 (oq, 8^1-CH_2), 3.65 (s, 12^1-CH_3), 3.13 (s, 1′-NCH_3), 3.12 (s, 7^1-CH_3), 2.74–2.50, 2.40–1.98 (m, 17^1-CH_2, 17^2-CH_2), 1.86 (d, $^3J = 7.3$ Hz, 18^1-CH_3), 1.69 (ot, 8^2-CH_3), −1.86 (br s, 23-N*H*) (21-N*H* is not resolved); UV-VIS (CH_2Cl_2), λ_{max} (rel absorbance) 316 (0.470), 412 (1.000), 512 (0.104), 542 (0.092), 615 (0.071), 668 (0.521); MALDI-TOF MS *m*/*z* 1284.30 (M + H$^+$) $C_{94}H_{37}O_3N_5$ requires 1283.29. *Atropisomer* **PF2**: ^{1}H NMR (300 MHz, $CDCl_3$–CD_3OD 40 : 1), *Epimer A*: δ_H 9.63 (s, 5-C*H*), 9.48 (s, 10-C*H*), 8.65 (s, 20-C*H*), 6.74 (s, 2′-C*H*), 5.28 (AX spin system, d, $|^2J| = 9.7$ Hz, 5′-CH_2), 5.24, 5.08 (AB spin system, $|^2J| = 20.1$ Hz, 13^2-CH_2), 4.55 (AX spin system, d, $|^2J| = 9.7$ Hz, 5′-CH_2), 4.51 (m, 18-C*H*), 4.31 (m, 17-C*H*), 3.97 (s, 2^1-CH_3), 3.72 (oq, 8^1-CH_2), 3.63 (s, 12^1-CH_3), 3.08 (s, 7^1-CH_3), 3.07 (s, 1′-NCH_3), 2.74–2.54, 2.40–2.01 (m, 17^1-CH_2, 17^2-CH_2), 1.80 (d, $^3J = 7.5$ Hz, 18^1-CH_3), 1.72 (ot, 8^2-CH_3), −1.74 (br s, 23-N*H*) (21-N*H* is not resolved); *Epimer B*: δ_H 11.34 (s, 5-C*H*), 9.51 (s, 10-C*H*), 8.57 (s, 20-C*H*), 6.35 (s, 2′-C*H*), 5.37 (AX spin system, d, $|^2J| = 9.7$ Hz, 5′-CH_2), 5.26, 5.10 (AB spin system, $|^2J| = 20.1$ Hz, 13^2-CH_2), 4.62 (AX spin system, d, $|^2J| = 9.7$ Hz, 5′-CH_2), 4.51 (m, 18-C*H*), 4.31 (m, 17-C*H*), 3.72 (oq, 8^1-CH_2), 3.66 (s, 12^1-CH_3), 3.53 (s, 2^1-CH_3), 3.40 (s, 7^1-CH_3), 2.95 (s, 1′-NCH_3), 2.74–2.54, 2.40–2.01 (m, 17^1-CH_2, 17^2-CH_2), 1.78 (d, $^3J = 7.5$ Hz, 18^1-CH_3), 1.72 (ot, 8^2-CH_3), −1.85 (br s, 23-N*H*) (21-N*H* is not resolved); UV-VIS (CH_2Cl_2), λ_{max} (rel absorbance) 316 (0.471), 412 (1.000), 512 (0.101), 542 (0.089), 615 (0.069), 668 (0.520); MALDI-TOF MS *m*/*z* 1284.30 (M + H$^+$), $C_{94}H_{37}O_3N_5$ requires 1283.29.

α,β-3-((2′*R*,*S*)-*N*-Methyltetrahydro[60]fullereno[*c*]*N*-methyl-pyrrol-2′-yl)-3-deethylphytochlorin methyl ester (6)

A solution of 26 mg of C_{60} (0.036 mmol) in 15 ml of dry toluene were added to a solution of 20 mg (0.036 mmol) of **3** and 16 mg (0.18 mmol) of *N*-methylglycine in 35 ml of dry toluene. The mixture obtained was refluxed under Ar and the progress of the reaction was monitored by TLC on Merck's Si-60 silica plates [thickness of the layer 0.25 mm; eluent $CHCl_3$–acetone 19 : 1 (v/v)]. After 24 h of reflux, the mixture was cooled to room temperature and the toluene was evaporated. The residue obtained was chromatographed on a silica gel column [230–400 mesh; height of the layer 280 mm; 300 × 45 mm ID column; elution with $CHCl_3$–acetone 20 : 1 (v/v)] to give pure dyads **6** (23 mg, 49% yield) as a mixture of two diastereomers and two atropisomers. ^{1}H NMR (500 MHz, $CDCl_3$–CS_2 1 : 1): δ_H 11.37, 11.35, 9.66, 9.66 (s, 5-C*H*), 9.56, 9.55, 9.53, 9.52 (s, 10-C*H*), 8.66, 8.65, 8.58, 8.58 (s, 20-C*H*), 6.73, 6.72, 6.33, 6.31 (s, 2′-C*H*), 5.38–5.30 (4H, AX spin system, overlapping doublets (od), 5′-CH_2), 5.30–5.02 (8H, AB spin system, 13^2-CH_2), 4.59, 4.50, 4.50, 4.50 (AX spin system, od, 5′-CH_2), 4.49 (4H, m, 18-C*H*), 4.29 (4H, m, 17-C*H*), 3.96, 3.95, 3.52, 3.51 (s, 2^1-CH_3), 3.72 (8H, oq, 8^1-CH_2), 3.69, 3.67, 3.66, 3.65 (s, 12^1-CH_3), 3.62, 3.61, 3.60, 3.59 (s, 17^4-CH_3), 3.40, 3.40, 3.12, 3.09 (s, 7^1-CH_3), 3.04, 3.03, 2.93, 2.90 (s, 1′-NCH_3), 2.74–2.48, 2.38–2.10 (16H, m, 17^1-CH_2, 17^2-CH_2), 1.88–1.75 (12H, od, 18^1-CH_3), 1.75–1.64 (12H, ot, 8^2-CH_3), 0.31 (4H, br s, 21-N*H*), −1.67, −1.73, −1.81, −1.82 (br s, 23-N*H*); UV-VIS (CH_2Cl_2), λ_{max} (rel absorbance) 317 (0.472), 413 (1.000), 511 (0.101), 541 (0.090), 613 (0.067), 669 (0.517); MS *m*/*z* 1298.27 (M + H$^+$), $C_{95}H_{39}O_3N_5$ requires 1297.30.

α,β-3-((2′*R*,*S*)-*N*-Methyltetrahydro[60]fullereno[*c*]pyrrol-2′-yl)-3-deethylphytochlorinato-Zn(II) methyl ester (7)

Compound **6** (10 mg, 0.008 mmol) was dissolved in 10 ml of dry $CHCl_3$ and 1.0 ml of saturated solution of $Zn(CH_3COO)_2$ in MeOH was added with stirring under Ar. The reaction mixture was refluxed for 3 h and the progress of the reaction was monitored by TLC on Merck's Si-60 silica plates [thickness of the layer 0.25 mm; eluent $CHCl_3$–acetone 19 : 1 (v/v)], cooled to room temperature and diluted with $CHCl_3$ (20 ml). The solution was then washed 3 times with water, dried over anhydrous Na_2SO_4 and evaporated to dryness on a rotary evaporator to yield 9 mg (86%) of pure dyad **6**. ^{1}H NMR (300 MHz, $CDCl_3$–CD_3OD 40 : 1): δ_H 11.28, 11.23, 9.51, 9.51 (s, 5-C*H*), 9.50, 9.48 (each 2H, s, 10-C*H*), 8.44, 8.44, 8.36, 8.35 (s, 20-C*H*), 6.67, 6.67, 6.28, 6.27 (s, 2′-C*H*), 5.42, 5.29 (each 2H, AX spin system, d, $|^2J| = 9.7$ Hz, 5′-CH_2), 5.10, 5.11, 4.96, 4.95 (each 2H, overlapping AB spin systems, $|^2J| = 20$ Hz, 13^2-CH_2), 4.61, 4.58 (each 2H, AX spin system, d, $|^2J| = 9.7$ Hz, 5′-CH_2), 4.41 (4H, m, 18-C*H*), 4.23 (4H, m, 17-C*H*), 3.86, 3.85, 3.56, 3.56 (s, 2^1-CH_3), 3.71 (8H, oq, 8^1-CH_2), 3.58, 3.57 (each 6H, s, 12^1-CH_3), 3.42, 3.40 (each 6H, s, 17^4-CH_3), 3.41, 3.25, 3.24, 3.20 (s, 7^1-CH_3), 3.13, 3.10, 3.03, 3.01 (s, 1′-NCH_3), 2.62–2.38, 2.24–1.98 (16H, m, 17^1-CH_2, 17^2-CH_2), 1.84–1.74 (12H, od, 18^1-CH_3),

1.74–1.64 (12H, ot, 8^2-CH_3); UV-VIS (CH_2Cl_2), λ_{max} (rel absorbance) 313 (0.541), 424 (1.000), 517 (0.033), 558 (0.049), 609 (0.098), 656 (0.705); MS *m*/*z* 1360.26 ($M + H^+$), $C_{95}H_{37}O_3N_5Zn$ requires 1359.22.

Acknowledgements

The authors thank Jari Helin (Institute of Biotechnology, University of Helsinki, Finland) for the MALDI-TOF spectra. Support from Technology Development Centre (TEKES), the Academy of Finland and Deutscher Akademischer Austauschdienst (DAAD) is acknowledged.

References

1 M. R. Wasielewski, *Chem. Rev.*, 1992, **92**, 435.
2 P. A. Liddell, J. P. Sumida, A. N. Macpherson, L. Noss, G. R. Seely, K. N. Clark, A. L. Moore, T. A. Moore and D. Gust, *Photochem. Photobiol*., 1994, **60**, 537.
3 T. Drovetskaya, C. A. Reed and P. Boyd, *Tetrahedron Lett.*, 1995, **36**, 7971.
4 H. Imahori, K. Yamada, M. Hasegawa, S. Taniguchi, T. Okada and Y. Sakata, *Angew. Chem.*, *Int. Ed. Engl.*, 1997, **36**, 2626.
5 J. R. Bolton, *Science*, 1978, **202**, 705.
6 J. R. Bolton, S. J. Strickler and J. S. Connolly, *Nature*, 1985, **316**, 495.
7 M. Gouterman, in *Optical Spectra and Electronic Structures of Porphyrins and Related Rings*, *The Porphyrins*, ed. D. Dolphin, Academic Press, New York, 1978, vol. 3, part A, pp. 1–165.
8 R. H. Felton, in *Primary Redox Reactions of Metalloporphyrins*, *The Porphyrins*, ed. D. Dolphin, Academic Press, New York, 1978, vol. 5, part C pp. 53–125.
9 A. Y. Tauber, R. K. Kostiainen and P. H. Hynninen, *Tetrahedron*, 1994, **50**, 4723.
10 D. G. Johnson, W. A. Svec and M. R. Wasielewski, *Isr. J. Chem.*, 1988, **28**, 193.
11 M. Maggini, G. Scorrano and M. Prato, *J. Am. Chem. Soc.*, 1993, **115**, 9798.
12 J. Helaja, A. Y. Tauber, I. Kilpeläinen and P. H. Hynninen, *Magn. Reson. Chem.*, 1997, **35**, 619.
13 K. M. Smith, D. A. Goff and D. J. Simpson, *J. Am. Chem. Soc.*, 1985, **107**, 4946.
14 M. Prato, T. Suzuki, F. Wudl, V. Lucchini and M. Maggini, *J. Am. Chem. Soc.*, 1993, **115**, 7876.
15 K. A. Connors, *Chemical Kinetics*, VCH Publishers, New York, 1990.
16 HYPERCHEM, Hypercube, http://www. hyper. com.
17 M. J. S. Dewar, E. G. Zoebisch and E. F. Healy, J. J. P. Stewart, *J. Am. Chem. Soc.*, 1985, **107**, 3902.
18 N. V. Tkachenko, L. Rantala, A. Y. Tauber, J. Helaja, P. H. Hynninen and H. Lemmetyinen, *J. Am. Chem. Soc.*, in the press.
19 P. H. Hynninen, *Acta Chem. Scand.*, 1977, **31B**, 829.

Paper 9/04817K